






Stability of the Pb divalent state in insulating and metallic PbCrO_3

Jianfa Zhao ^{1,*}, Shu-Chih Haw,^{2,†} Xiao Wang ³, Lipeng Cao,⁴ Hong-Ji Lin,² Chien-Te Chen ², Christoph J. Sahle,⁵ Arata Tanaka ⁶, Jin-Ming Chen,² Changqing Jin,^{1,7} Zhiwei Hu,^{3,‡} and Liu Hao Tjeng ^{3,§}

¹Beijing National Laboratory for Condensed Matter Physics, Institute of Physics, Chinese Academy of Sciences, Beijing 100190, China

²National Synchrotron Radiation Research Center, 101 Hsin-Ann Road, Hsinchu 30076, Taiwan

³Max-Planck Institute for Chemical Physics of Solids, Nothnitzer Straße 40, 01187 Dresden, Germany

⁴State Key Laboratory of Materials Science & Technology and Key Laboratory for Microstructural Material Physics of Hebei Province, School of Science, Yanshan University, Qinhuangdao, Hebei 066004, China

⁵European Synchrotron Radiation Facility (ESRF), 71 Avenue des Martyrs, Grenoble 38000, France

⁶Department of Quantum Matter, ADSM, Hiroshima University, Higashi-Hiroshima 739-8530, Japan

⁷School of Physics Sciences, University of Chinese Academy of Sciences, Beijing 100190, China



(Received 9 November 2022; accepted 13 January 2023; published 26 January 2023)

We have investigated the local electronic structure of PbCrO_3 by conducting x-ray absorption spectroscopy at the lead L_3 and chromium $L_{2,3}$ edges. We found that lead is divalent and chromium is charge-disproportionated into trivalent and hexavalent states at ambient pressures, explaining their insulating behavior. The high-resolution partial fluorescence yield of lead L_3 spectra as a function of pressure revealed that the divalent state of lead ions remains unchanged at high pressures, when PbCrO_3 changes into metal and its volume collapses by more than 10%. We infer that the insulator-to-metal transition does not involve a Pb-Cr charge transfer, but is associated with the conversion of $\text{Cr}^{3+}/\text{Cr}^{6+}$ charge-disproportionated states into a Cr^{4+} valence state.

DOI: [10.1103/PhysRevB.107.024107](https://doi.org/10.1103/PhysRevB.107.024107)

I. INTRODUCTION

PbCrO_3 is an antiferromagnetic insulator with a Néel temperature of about $T_N = 240$ K and is believed to exhibit a cubic perovskite crystal structure [1–3]. It has also been recently discovered to undergo a large volume collapse of more than 9.8% [4], and concurrently, an insulator-to-metal transition [5,6], at a pressure of ~ 1.6 GPa. The following aspects make PbCrO_3 intriguing: (i) Why is PbCrO_3 an insulator at ambient pressures? (ii) What is the mechanism behind the insulator-to-metal transition under pressure?

Numerous band structure studies have been conducted to determine the electronic structure of the cubic perovskite PbCrO_3 and all found a metallic solution [7–10], which disagrees with the experimentally observed insulating state at ambient pressures. Even the inclusion of the Hubbard U in the calculations to account for electron correlation effects did not resolve the problem [8–10]. In fact, this fits to the experimental observation that all Cr^{4+} oxides with octahedral

coordination exhibit the tendency to be metallic [11–15]. This phenomenon can be related to the heavily negative oxygen $2p$ to chromium $3d$ charge transfer energy [16–18] that pins the chemical potential inside the oxygen band [11].

A microstructure study [19] provided the first indications that the crystal structure might be more complicated than the widely accepted pure cubic perovskite PbCrO_3 . Assuming, for example, that CrPbO_3 is present in the material, one could arrive at an insulating solution in band structure calculations [9]. Valuable insight was gained from x-ray absorption spectroscopy (XAS) at the chromium $L_{2,3}$ edges, revealing the presence of charge disproportionation of chromium ions into Cr^{3+} and Cr^{6+} configurations at ambient pressures [20]. A careful analysis of neutrons and x-ray diffraction (XRD) data showed anomalously large thermal factors of the lead, chromium, and oxygen ions [6], motivating the proposal of the chromium charge-disproportionated state that will allow density functional theory to produce an insulating state for moderate values of the Hubbard U . The metallic high-pressure phase is the result of lifting the charge disproportionation situation into a phase in which all chromium elements become tetravalent [6]. Another study proposed that lead ions are charge-disproportionated into Pb^{2+} and Pb^{4+} , and that all chromium ions are Cr^{3+} at ambient pressures [21]. Accordingly, the high-pressure phase is a transformation that involves a Pb-Cr charge transfer into homogenous Pb^{2+} and Cr^{4+} valence configurations. Recently, unusual lattice elasticity properties have also been observed [22] across the volume collapse and insulator-to-metal transition.

We followed a complementary route of research to understand the peculiar properties of PbCrO_3 and to resolve

*zhaojf@iphy.ac.cn

†ho.kelman@nsrrc.org.tw

‡zhiwei.hu@cpfs.mpg.de

§hao.tjeng@cpfs.mpg.de

the debate about the origin of insulator-to-metal transition. We aimed to determine lead valence spectroscopically under ambient and high-pressure conditions. To achieve this objective, we used known information about the PbMO_3 ($M = 3d$ transition metal) series [23–25]. PbMO_3 undergoes a sequence of transitions in electronic configuration across the $3d$ transition metal row from left to right in the periodic table. The valence state gradually evolves from $+2/+4$ to $+4/+2$ for Pb/M ions—namely, from $\text{Pb}^{2+}M^{4+}\text{O}_3$ ($M = \text{Ti}, \text{V}$) [26,27] to $\text{Pb}_{0.5}^{2+}\text{Pb}_{0.5}^{4+}\text{Fe}^{3+}\text{O}_3$ [28], and further to $\text{Pb}^{4+}\text{Ni}^{2+}\text{O}_3$ [29]. Manganese and cobalt ions in the middle of the series exhibit a complicated mixed valence state—namely, $\text{Pb}_{0.875}^{2+}\text{Pb}_{0.125}^{4+}\text{Mn}_{0.25}^{3+}\text{Mn}_{0.75}^{4+}\text{O}_3$ [30] and $\text{Pb}_{0.25}^{2+}\text{Pb}_{0.75}^{4+}\text{Co}_{0.5}^{2+}\text{Co}_{0.5}^{3+}\text{O}_3$ [31,32], respectively. From this series, one may infer that Pb^{2+} valence is likely for PbCrO_3 , but also that Pb^{4+} state cannot be excluded. In the current study, we used bulk-sensitive lead L_3 XAS by measuring the signal in the transmission mode by using the high-resolution partial fluorescence yield (PFY) mode [28,30,32–35]. We compared the spectra of our PbCrO_3 with those of PbTiO_3 and PbNiO_3 . This experiment was accompanied with a detailed XRD and chromium $L_{2,3}$ XAS investigation of our PbCrO_3 sample.

II. EXPERIMENTAL

Polycrystalline samples of PbCrO_3 were synthesized via a solid-state reaction under high pressure and high temperature of 1273 K. The starting materials PbO (Aldrich, 99.0% pure) and CrO_2 (Alfa, 99.995% pure) were mixed homogeneously in accordance with a molar ratio of 1:1 and sealed in a gold capsule with a diameter of 2 mm. High-pressure experiments were performed in a Walker-type multianvil module (Rockland Research Co.). After pressure was gradually increased to 15 GPa, the system was heated to 1273 K within 10 min, and this temperature was maintained for 30 min. Then, the temperature was quenched to room temperature before releasing the pressure. After the high-pressure and high-temperature process, polycrystalline PbCrO_3 was obtained.

Sample quality and crystal structure were characterized via powder XRD using a Huber diffractometer with wavelength $\lambda = 1.5406 \text{ \AA}$ (copper $K_{\alpha 1}$ radiation, 40 kV, 30 mA). Diffraction data were collected in the angle (2θ) range from 10° to 100° , with steps of 0.005° . XRD data were analyzed by using the Rietveld refinement program GSAS [36]. The high-resolution PFY lead L_3 XAS spectra with an overall experimental resolution of ~ 2.5 eV were collected at the ID 20 beamline of the European Synchrotron Radiation Facility in France [37]. The PbTiO_3 and PbNiO_3 samples were also measured to serve as Pb^{2+} ($6s^2$) and Pb^{4+} ($6s^0$) reference materials, respectively. The chromium $L_{2,3}$ XAS spectra of PbCrO_3 together with Cr_2O_3 as a Cr^{3+} reference and $\text{Ag}_2\text{Cr}_2\text{O}_7$ as a Cr^{6+} reference were measured at BL11A of the National Synchrotron Radiation Research Center in Taiwan.

III. RESULTS AND DISCUSSION

The experimental XRD pattern of PbCrO_3 collected at room temperature is shown in Fig. 1. In the beginning, the XRD pattern was simulated with a cubic $Pm\text{-}3m$ perovskite

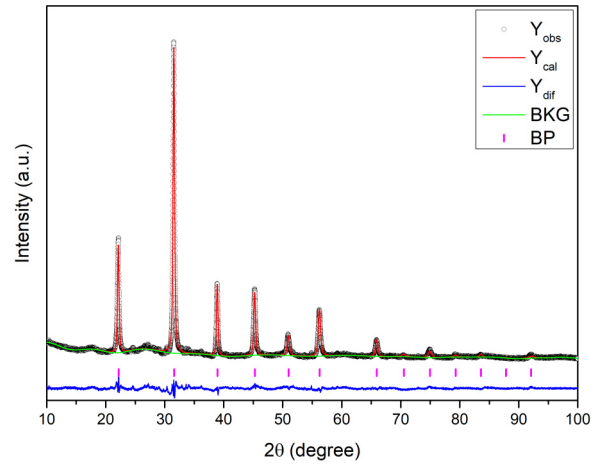


FIG. 1. Rietveld structural refinement of the XRD pattern for PbCrO_3 collected at 300 K using the $\text{Cr}^{3+}/\text{Cr}^{6+}$ charge disproportionation model. Observed (crosses), calculated (red), and difference (blue) are shown in the figure. The R_{wp} , R_p , and χ^2 are 3.89%, 3.35%, and 4.276. The ticks indicate the allowed Bragg reflections of PbCrO_3 with the charge disproportionation model.

structure model that provided reliability factors $R_{wp} = 3.66\%$, $R_p = 3.16\%$, and $\chi^2 = 4.103$. However, the isotropic thermal factor B_{iso} of the lead, chromium, and oxygen sites exhibited abnormally high values: $B_{\text{iso}}(\text{Pb}) = 8.95(2) \text{ \AA}^2$, $B_{\text{iso}}(\text{Cr}) = 6.77(5) \text{ \AA}^2$, and $B_{\text{iso}}(\text{O}) = 6.7(1) \text{ \AA}^2$. These findings are similar to those of Cheng *et al.* [6]. We also conducted simulations with the thermal factors fixed to reasonable values. We determined that the reliability factors rapidly increased to $R_{wp} = 9.87\%$, $R_p = 7.62\%$, and $\chi^2 = 12.28$. These findings indicate that the cubic perovskite structure model is inaccurate.

Following the interpretation of Cheng *et al.* [6], we also considered the charge disproportionation scenario as follows: the lead, chromium, and oxygen atoms are allowed to be off from the $(0, 0, 0)$, $(0.5, 0.5, 0.5)$, and $(0, 0.5, 0.5)$ positions and, instead, they occupy the general Wyckoff sites $8g$ ($0.0619, 0.0619, 0.0619$), $8g$ ($0.5442, 0.5442, 0.5442$), and $24m$ ($0.0489, 0.5348, 0.5348$), respectively. With this new structural model, the thermal factor dropped significantly to $1.70(3) \text{ \AA}^2$, $2.95(6) \text{ \AA}^2$, and $3.7(1) \text{ \AA}^2$ for lead, chromium, and oxygen, respectively, providing reliability factors $R_{wp} = 3.89\%$, $R_p = 3.35\%$, and $\chi^2 = 4.276$, and the lattice constant ($a = 4.0043 \text{ \AA}$) in accordance with previous reports [1,3,4,6,19–21]. Figure 1 displays this refinement model with charge disproportionation and shows that all XRD peaks are reproduced well, indicating that our PbCrO_3 sample prepared under 15 GPa exhibits no evident impurity phases [1,6,19].

Figure 2 presents the PFY lead L_3 XAS spectrum of PbCrO_3 , along with those of PbTiO_3 (as Pb^{2+} reference) and PbNiO_3 (as Pb^{4+} reference). The sharp pre-edge peak at 13 043 eV in the lead L_3 XAS spectrum for the Pb^{4+} reference PbNiO_3 can be assigned to the dipole-allowed transition from the $2p_{3/2}$ core level to the fully unoccupied $6s$ shell. By contrast, in the case of PbTiO_3 , the pre-edge peak is absent due to the fully occupied $6s$ shell. Figure 2 shows that PbCrO_3 has a lead L_3 XAS profile similar to that of PbTiO_3 . Only a more broader shoulder A at the leading edge (13 047 eV)

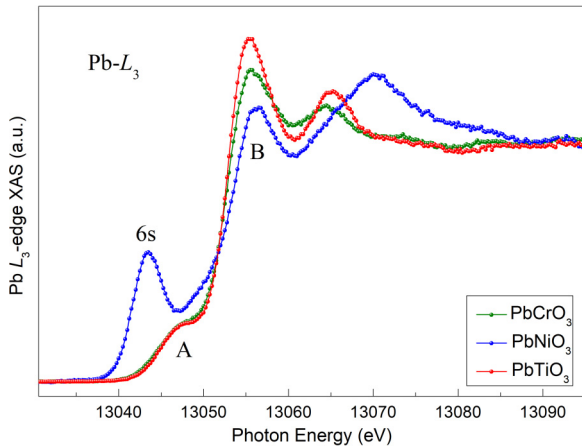


FIG. 2. High-resolution XAS spectra at the lead L_3 edge of PbCrO_3 and PbTiO_3 (as Pb^{2+} reference) and PbNiO_3 (as Pb^{4+} reference).

was observed in both Pb^{2+} oxides PbCrO_3 and PbTiO_3 . This shoulder A at the leading edge is related to the lowest lead $6d$ state above Fermi energy, which is mixed with lead $6p$ and oxygen $2p$ [38]. The lack of a pre-edge peak in PbCrO_3 thus establishes that the lead ion is in the divalent state. This result contradicts the assessment of Yu *et al.* [21] who proposed that lead ions are charge-disproportionated into Pb^{2+} and Pb^{4+} at ambient pressures.

Having determined the divalent state of the lead ion, we must now confirm that chromium is, on average, tetravalent to fulfill the charge balance requirement. The energy position and line shape of the $3d$ transition-metal $L_{2,3}$ XAS spectra are well known to be highly sensitive to the valence and local environment of the ion [39–42]. In case of a mixed valence material, its spectrum can be obtained by the superposition of some related components [43]. In Fig. 3(a), we present the chromium $L_{2,3}$ XAS spectrum of PbCrO_3 . This spectrum is extremely different from that of a Cr^{4+} ion that is coordinated octahedrally by oxygen atoms [41,42]. To interpret the spectrum, we also plot in Fig. 3(a) the experimental spectrum of Cr_2O_3 (red curve) as a Cr^{3+} reference material with CrO_6 octahedral coordination, and that of $\text{Ag}_2\text{Cr}_2\text{O}_7$ (green curve) as a Cr^{6+} reference material with CrO_4 tetrahedral coordination [44]. We then construct a superposition of the Cr_2O_3 and $\text{Ag}_2\text{Cr}_2\text{O}_7$ spectra with $2/3$ and $1/3$ weights, respectively. We can observe that this superposition (blue curve) reproduces the experimental spectrum of PbCrO_3 . Although the PbCrO_3 spectrum of Wu *et al.* [20] contains somewhat too much Cr^{6+} signal, we can state that we essentially reproduce their chromium $L_{2,3}$ XAS analysis. Therefore, we can conclude that a $\text{Cr}^{3+}/\text{Cr}^{6+}$ charge disproportionation of chromium occurs in PbCrO_3 at ambient pressures as proposed by Wu *et al.* [20] and Cheng *et al.* [6]. Notably, the $2/3$ Cr^{3+} and $1/3$ Cr^{6+} weights used for the superposition imply that the average valence of chromium is $+4$, completely fulfilling the charge balance, with lead being divalent.

To obtain a deeper understanding of the local electronic structure of the chromium ion in PbCrO_3 , we performed cluster calculations that included full atomic multiplet interactions, local ionic crystal field splitting, and oxygen

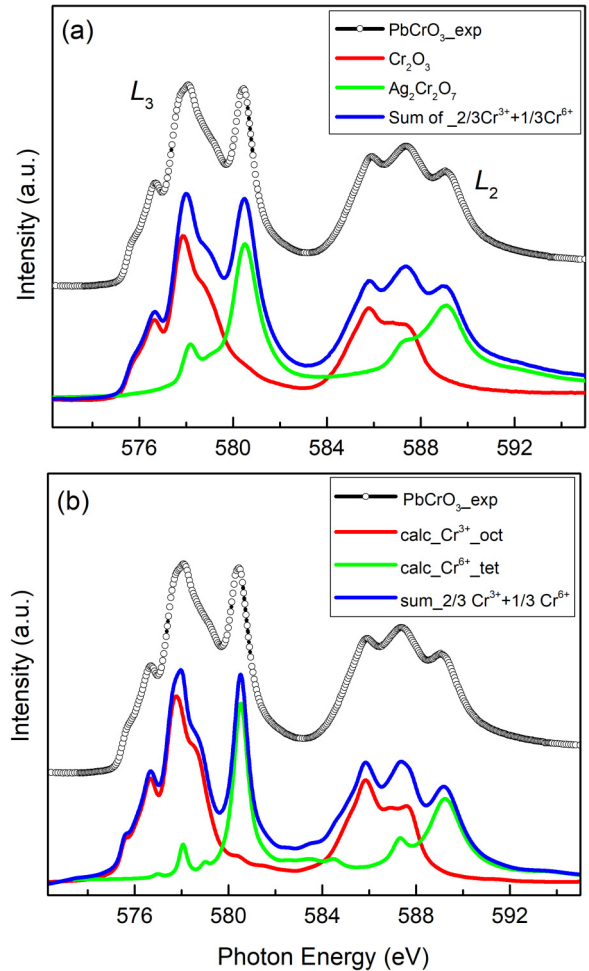


FIG. 3. (a) Chromium $L_{2,3}$ XAS experimental spectra of PbCrO_3 (black circles) and sum (blue line) of Cr^{3+} reference Cr_2O_3 and Cr^{6+} reference $\text{Ag}_2\text{Cr}_2\text{O}_7$ in a 2:1 ratio. (b) Calculated chromium $L_{2,3}$ XAS of Cr^{3+} in octahedral coordination (red line), Cr^{6+} in tetrahedral coordination (green line), and the sum of them in a 2:1 ratio (blue line).

$2p$ -chromium $3d$ hybridization. The calculations were performed using XTLS 9.0 code [45]. We used an octahedral CrO_6 cluster for Cr^{3+} and a tetrahedral CrO_4 cluster for Cr^{6+} . (The parameter values, in electron volts, are as follows: octahedral Cr^{3+} O_6 cluster: $U_{dd} = 5.5$, $U_{cd} = 7.0$, $\Delta = 5.0$, $10Dq = 1.15$, Slater integrals set at 75% of the Hartree-Fock values; tetrahedral Cr^{6+} O_4 cluster: $U_{dd} = 5.5$, $U_{cd} = 7.0$, $\Delta = -4.0$, $10Dq = 0.35$, Slater integrals set at 70% of the Hartree-Fock values.) As displayed in Fig. 3(b), we are able to reproduce excellently the spectra of Cr_2O_3 , $\text{Ag}_2\text{Cr}_2\text{O}_7$, and PbCrO_3 , confirming our experimental conjectures. Here, we like to stress that we have used a tetrahedral coordination for Cr^{6+} calculations. Our modeling is related to the empirical observation that extremely high-valent chromium oxides (pentavalent and hexavalent) have chromium ions that are not octahedrally, but tetrahedrally, coordinated. A combined experimental and theoretical study on YCrO_4 found that tetrahedral coordination can still stabilize an insulating state for high-valent chromium oxides while an octahedral coordination cannot [46]. This finding, along with the notion that a

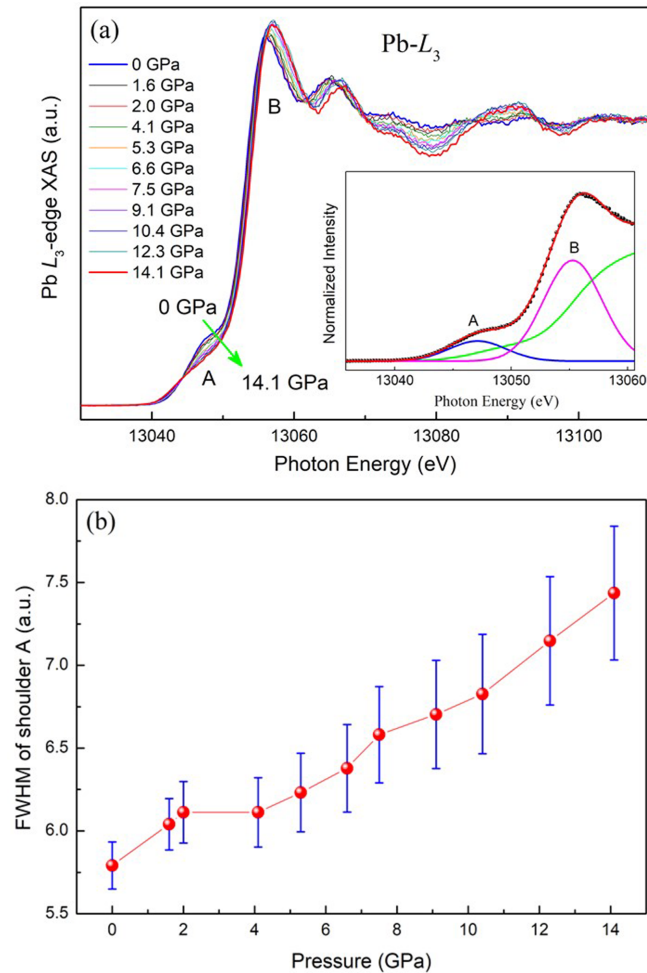


FIG. 4. (a) High-resolution XAS spectra at the lead L_3 edge of PbCrO_3 as a function of pressure from 0 GPa to 14.1 GPa. The inset shows the simulation of the lead L_3 XAS spectrum at 0 GPa. (b) Pressure-dependent FWHM of shoulder A.

Cr^{3+} oxide is readily a Mott insulator, such as Cr_2O_3 , provide the necessary ingredients for PbCrO_3 to become an insulator. Through these $\text{Cr}^{3+}/\text{Cr}^{6+}$ charge disproportionation band structure calculations, one can find an insulating solution for modest and realistic values of the Hubbard U [6]. Moreover, the quasi-tetrahedral coordination of the Cr^{6+} ion proposed in a previous study [6] explains why the crystal structure cannot be described as a pure, undistorted cubic perovskite.

We then investigate what happens with lead valence when pressure is applied. Figure 4(a) shows the high-resolution PFY XAS spectra at the lead L_3 edge of PbCrO_3 over a wide

range of pressures—namely, from 0 GPa to 14.1 GPa—i.e., from the insulating phase under ambient conditions to deep inside the volume-collapsed metallic state. We do not observe a pre-edge peak in all the instances. This result shows that the valence state of the lead ions in PbCrO_3 always remains divalent. That is, our pressure-dependent PFY lead L_3 XAS results show that no relevant Pb-to-Cr charge transfer occurs in PbCrO_3 , contradicting the assertions of Yu *et al.* [21]. Moreover, we observe in Fig. 4(a) a systematic variation of the lower energy shoulder A with pressure. To be quantitative, we analyze the spectra by simulating its components. As an example, we show in the inset, the analysis for the 0-GPa spectrum. The curve with the black dots is the experiment, the blue line represents the shoulder A, while the magenta and green lines stand for the main unoccupied lead $6d$ state [38] and the continuum edge, respectively. We have done the simulation for all pressures. The full width at half maximum (FWHM) of shoulder A as a function of pressure is presented in Fig. 4(b). We can observe that the FWHM of shoulder A increases from 5.8 at 0 GPa to 7.4 at 14.1 GPa. This indeed indicates an increase in the bandwidth of the lowest lead $6d$ with pressure, reflecting the pressure-induced insulator-metal transition.

IV. CONCLUSIONS

We found evidence from our high-resolution PFY XAS at the lead L_3 edges and soft XAS at the chromium $L_{2,3}$ edges for the divalent state of lead ions and the occurrence of $\text{Cr}^{3+}/\text{Cr}^{6+}$ charge disproportionation in PbCrO_3 at ambient pressures. This charge disproportionation, along with the tetrahedral coordination of high-valent chromium, provide the necessary ingredients to form the insulating state and explain the presence of large lattice distortions away from the ideal cubic perovskite. The stability of the Pb^{2+} state as a function of pressure indicates that volume collapse and insulator-to-metal transition are not connected to Pb-to-Cr charge transfer, but rather to the suppression of the chromium charge disproportionation and the appearance of octahedrally coordinated tetravalent chromium.

ACKNOWLEDGMENTS

The work was supported by the Natural Science Foundation of China (Grant No. 12204515). We acknowledge the support from the Max Planck-POSTECH-Hsinchu Center for Complex Phase Materials. We also acknowledge the European Synchrotron Radiation Facility and National Synchrotron Radiation Research Center (NSRRC) in Taiwan for provision of synchrotron radiation facilities and technical support at beamline ID20 and BL11A, respectively.

- [1] W. L. Roth and R. C. Devries, Crystal and magnetic structure of PbCrO_3 , *J. Appl. Phys.* **38**, 951 (1967).
- [2] R. C. Devries and W. L. Roth, High-pressure synthesis of PbCrO_3 , *J. Am. Ceram. Soc.* **51**, 72 (1968).
- [3] B. Chamberland and C. Moeller, A study on the PbCrO_3 perovskite, *J. Solid State Chem.* **5**, 39 (1972).

- [4] W. S. Xiao, D. Y. Tan, X. L. Xiong, J. Liu, and J. A. Xu, Large volume collapse observed in the phase transition in cubic PbCrO_3 perovskite, *Proc. Natl. Acad. Sci. USA* **107**, 14026 (2010).
- [5] W. D. Wang, D. W. He, W. S. Xiao, S. M. Wang, and J. A. Xu, Electrical characterization in the phase transition between

- cubic PbCrO_3 perovskites at high pressures, *Chin. Phys. Lett.* **30**, 117201 (2013).
- [6] J. G. Cheng, K. E. Kweon, S. A. Larregola, Y. Ding, Y. Shirako, L. G. Marshall, Z. Y. Li, X. Li, A. M. dos Santos, M. R. Suchomel, K. Matsubayashi, Y. Uwatoko, G. S. Hwang, J. B. Goodenough, and J. S. Zhou, Charge disproportionation and the pressure-induced insulator-metal transition in cubic perovskite PbCrO_3 , *Proc. Natl. Acad. Sci. USA* **112**, 1670 (2015).
- [7] S. M. Jaya, R. Jagadish, R. Rao, and R. Asokamani, Electronic structure of the perovskite oxides SrCrO_3 and PbCrO_3 , *Mod. Phys. Lett. B* **6**, 103 (1992).
- [8] P. Ganesh and R. Cohen, Orbital ordering, ferroelasticity, and the large pressure-induced volume collapse in PbCrO_3 , *Phys. Rev. B* **83**, 172102 (2011).
- [9] B. T. Wang, W. Yin, W. D. Li, and F. Wang, First-principles study of pressure-induced phase transition and electronic property of PbCrO_3 , *J. Appl. Phys.* **111**, 013503 (2012).
- [10] Y. Lu, D. He, F. Peng, and X. Cheng, The mystery of abnormally large volume of PbCrO_3 with a structurally consistent Hubbard U from first-principles, *Eur. Phys. J. B* **86**, 1 (2013).
- [11] M. Korotin, V. Anisimov, D. Khomskii, and G. Sawatzky, CrO_2 : A Self-Doped Double Exchange Ferromagnet, *Phys. Rev. Lett.* **80**, 4305 (1998).
- [12] J. S. Zhou, C. Q. Jin, Y. W. Long, L. X. Yang, and J. Goodenough, Anomalous Electronic State in CaCrO_3 and SrCrO_3 , *Phys. Rev. Lett.* **96**, 046408 (2006).
- [13] L. Ortega-San-Martin, A. J. Williams, J. Rodgers, J. P. Attfield, G. Heymann, and H. Huppertz, Microstrain Sensitivity of Orbital And Electronic Phase Separation in SrCrO_3 , *Phys. Rev. Lett.* **99**, 255701 (2007).
- [14] A. Komarek, S. Streltsov, M. Isobe, T. Möller, M. Hoelzel, A. Senyshyn, D. Trots, M. Fernández-Díaz, T. Hansen, and H. Gotou, CaCrO_3 : An Anomalous Antiferromagnetic Metallic Oxide, *Phys. Rev. Lett.* **101**, 167204 (2008).
- [15] A. Komarek, T. Möller, M. Isobe, Y. Drees, H. Ulbrich, M. Azuma, M. Fernandez-Diaz, A. Senyshyn, M. Hoelzel, and G. André, Magnetic order, transport and infrared optical properties in the ACrO_3 system ($A = \text{Ca}, \text{Sr}, \text{and Pb}$), *Phys. Rev. B* **84**, 125114 (2011).
- [16] J. Zaanen, G. Sawatzky, and J. Allen, Band Gaps and Electronic Structure of Transition-Metal Compounds, *Phys. Rev. Lett.* **55**, 418 (1985).
- [17] J. B. Torrance, P. Lacorre, C. Asavaroengchai, and R. M. Metzger, Why are some oxides metallic, while most are insulating? *Physica C* **182**, 351 (1991).
- [18] D. Huang, L. Tjeng, J. Chen, C. Chang, W. Wu, S. Chung, A. Tanaka, G. Guo, H. J. Lin, and S. Shyu, Anomalous spin polarization and dualistic electronic nature of CrO_2 , *Phys. Rev. B* **67**, 214419 (2003).
- [19] A. M. Arevalo-Lopez and M. A. Alario-Franco, On the structure and microstructure of " PbCrO_3 ", *J. Solid State Chem.* **180**, 3271 (2007).
- [20] M. Wu, L. R. Zheng, S. Q. Chu, Z. X. Qin, X. J. Chen, C. L. Lin, Z. Tang, and T. D. Hu, Pressure-induced valence change and semiconductor-metal transition in PbCrO_3 , *J. Phys. Chem. C* **118**, 23274 (2014).
- [21] R. Z. Yu *et al.*, Melting of Pb charge glass and simultaneous Pb-Cr charge transfer in PbCrO_3 as the origin of volume collapse, *J. Am. Chem. Soc.* **137**, 12719 (2015).
- [22] S. M. Wang, J. Chen, L. S. Wu, and Y. S. Zhao, Giant Viscoelasticity Near Mott Criticality in PbCrO_3 With Large Lattice Anomalies, *Phys. Rev. Lett.* **128**, 095702 (2022).
- [23] J. B. Goodenough and J. S. Zhou, Varied roles of Pb in transition-metal PbMO_3 perovskites ($M = \text{Ti}, \text{V}, \text{Cr}, \text{Mn}, \text{Fe}, \text{Ni}, \text{Ru}$), *Sci. Technol. Adv. Mat.* **16**, 036003 (2015).
- [24] M. Azuma, Y. Sakai, T. Nishikubo, M. Mizumaki, T. Watanuki, T. Mizokawa, K. Oka, H. Hojo, and M. Naka, Systematic charge distribution changes in Bi- and Pb-3d transition metal perovskites, *Dalton Trans.* **47**, 1371 (2018).
- [25] K. Chen, Y. Mijiti, S. Agrestini, S. C. Liao, X. Li, J. Zhou, A. Di Cicco, F. Baudelet, L. H. Tjeng, and Z. Hu, Valence state of Pb in transition metal perovskites PbTMO_3 ($\text{TM} = \text{Ti}, \text{Ni}$) determined from X-ray absorption near-edge spectroscopy, *Phys. Status Solidi B* **255**, 1800014 (2018).
- [26] R. V. Shpanchenko, V. V. Chernaya, A. A. Tsirlin, P. S. Chizhov, D. E. Sklovsky, E. V. Antipov, E. P. Khlybov, V. Pomjakushin, A. M. Balagurov, J. E. Medvedeva, E. E. Kaul, and C. Geibel, Synthesis, structure, and properties of new perovskite PbVO_3 , *Chem. Mater.* **16**, 3267 (2004).
- [27] A. A. Belik, M. Azuma, T. Saito, Y. Shimakawa, and M. Takano, Crystallographic features and tetragonal phase stability of PbVO_3 , a new member of PbTiO_3 family, *Chem. Mater.* **17**, 269 (2005).
- [28] X. B. Ye *et al.*, Observation of novel charge ordering and spin reorientation in perovskite oxide PbFeO_3 , *Nat. Commun.* **12**, 1917 (2021).
- [29] Y. Inaguma, K. Tanaka, T. Tsuchiya, D. Mori, T. Katsumata, T. Ohba, K. Hiraki, T. Takahashi, and H. Saitoh, Synthesis, structural transformation, thermal stability, valence state, and magnetic and electronic properties of PbNiO_3 with perovskite- and LiNbO_3 -type structures, *J. Am. Chem. Soc.* **133**, 16920 (2011).
- [30] X. Li, Z. W. Hu, Y. J. Cho, X. Y. Li, H. Sun, L. Z. Cong, H. J. Lin, S. C. Liao, C. T. Chen, A. Efimenko, C. J. Sahle, Y. W. Long, C. Q. Jin, M. C. Downer, J. B. Goodenough, and J. S. Zhou, Charge disproportionation and complex magnetism in a PbMnO_3 perovskite synthesized under high pressure, *Chem. Mater.* **33**, 92 (2021).
- [31] Y. Sakai *et al.*, A-site and B-site charge orderings in an s - d level controlled perovskite oxide PbCoO_3 , *J. Am. Chem. Soc.* **139**, 4574 (2017).
- [32] Z. H. Liu *et al.*, Sequential spin state transition and intermetallic charge transfer in PbCoO_3 , *J. Am. Chem. Soc.* **142**, 5731 (2020).
- [33] J. Y. Yang, J. H. Dai, Z. H. Liu, R. Z. Yu, H. Hojo, Z. W. Hu, T. Pi, Y. Soo, C. Q. Jin, M. Azuma, and Y. W. Long, High-pressure synthesis of the cobalt pyrochlore oxide $\text{Pb}_2\text{Co}_2\text{O}_7$ with large cation mixed occupancy, *Inorg. Chem.* **56**, 11676 (2017).
- [34] J. F. Zhao *et al.*, Magnetic ordering and structural transition in the ordered double-perovskite $\text{Pb}_2\text{NiMoO}_6$, *Chem. Mater.* **34**, 97 (2021).
- [35] J. F. Zhao *et al.*, A combinatory ferroelectric compound bridging simple ABO_3 and A-site-ordered quadruple perovskite, *Nat. Commun.* **12**, 747 (2021).
- [36] B. H. Toby, EXPGUI, a graphical user interface for GSAS, *J. Appl. Crystallogr.* **34**, 210 (2001).
- [37] M. Moretti Sala, K. Martel, C. Henriquet, A. Al Zein, L. Simonelli, C. Sahle, H. Gonzalez, M. C. Lagier, C. Ponchut, and S. Huotari, A high-energy-resolution resonant inelastic

- X-ray scattering spectrometer at ID20 of the European Synchrotron Radiation Facility, *J. Synchrotron Radiat.* **25**, 580 (2018).
- [38] J. C. Swarbrick, U. Skyllberg, T. Karlsson, and P. Glatzel, High energy resolution X-ray absorption spectroscopy of environmentally relevant lead (II) compounds, *Inorg. Chem.* **48**, 10748 (2009).
- [39] C. Chen and F. Sette, High resolution soft x-ray spectroscopies with the Dragon beamline, *Phys. Scripta.* **T31**, 119 (1990).
- [40] F. M. de Groot, J. Fuggle, B. Thole, and G. Sawatzky, $2p$ X-ray absorption of $3d$ transition-metal compounds: An atomic multiplet description including the crystal field, *Phys. Rev. B* **42**, 5459 (1990).
- [41] D. Huang, H. T. Jeng, C. Chang, G. Guo, J. Chen, W. Wu, S. Chung, S. Shyu, C. Wu, and H. J. Lin, Orbital magnetic moments of oxygen and chromium in CrO_2 , *Phys. Rev. B* **66**, 174440 (2002).
- [42] G. X. Liu, Z. H. Liu, Y. S. Chai, L. Zhou, X. D. Shen, X. B. Ye, S. J. Qin, D. B. Lu, Z. W. Hu, L. H. Tjeng, H. J. Lin, C. T. Chen, X. H. Yu, and Y. W. Long, Magnetic and electric field dependent anisotropic magnetoelectric multiferroicity in $\text{SmMn}_3\text{Cr}_4\text{O}_{12}$, *Phys. Rev. B* **104**, 054407 (2021).
- [43] J. Chen, X. Wang, Z. W. Hu, L. H. Tjeng, S. Agrestini, M. Valvidares, K. Chen, L. Nataf, F. Baudelet, M. Nagao, Y. Inaguma, A. A. Belik, Y. Tsujimoto, Y. Matsushita, T. Kolodiaznyi, R. Sereika, M. Tanaka, and K. Yamaura, Enhanced magnetization of the highest- T_C ferrimagnetic oxide $\text{Sr}_2\text{CrOsO}_6$, *Phys. Rev. B* **102**, 184418 (2020).
- [44] A. Durif and M. Averbuch-Pouchot, Structure du dichromate d'argent: $\text{Ag}_2\text{Cr}_2\text{O}_7$, *Acta Crystallogr. B* **34**, 3335 (1978).
- [45] A. Tanaka and T. Jo, Resonant $3d$, $3p$ and $3s$ photoemission in transition-metal oxides predicted at $2p$ threshold, *J. Phys. Soc. Jpn.* **63**, 2788 (1994).
- [46] A. Tsirlin, M. Rabie, A. Efimenko, Z. W. Hu, R. Saez-Puche, and L. H. Tjeng, Importance of tetrahedral coordination for high-valent transition-metal oxides: YCrO_4 as a model system, *Phys. Rev. B* **90**, 085106 (2014).